geoconvention
Calgary • Canada • May 12-14 2025

Simultaneous FWI of geophone and fiberoptic data: Benefits and Challenges

Anton H. Ziegon, Kristopher A. Innanen
CREWES, University of Calgary

Summary

Frequency-dependent DAS and geophone data inclusion in elastic full-waveform inversion (EFWI) has the potential to tackle issues related to the cycle-skipping phenomenon. Cycle-skipping originates from a lack of low-wavenumber information of the subsurface, i.e. a lack of transmission or low-frequency data. Fiberoptic sensing is an affordable technology that can provide a cost-effective way to provide this wavefield information, however a simultaneous inversion of DAS and geophone data also poses challenges. In this work a framework is introduced to include both data types within EFWI and the effects of data importance weighting and data balancing are demonstrated using a simple synthetic model.

Introduction

The subsurface energy industry requires cost-effective and reliable seismic monitoring to ensure effectiveness and safety of projects. Elastic full-waveform inversion (EFWI) has been proven to be a valuable tool as it can recover elastic subsurface models with higher resolution than conventional post-stack images and therefore provide a more detailed reservoir description (Tarantola, 1984a,b; Tarantola, 1986). A common issue associated with EFWI is cycle-skipping, a phenomenon that arises from the convexity of the data misfit functional and results in modelled and observed data being out of phase (Virieux and Operto, 2009). Increasing low-wavenumber information in form of transmission wave recordings or low-frequency data was proven to mitigate the problem (Bunks et al., 1995), however, it is challenging to get these data types from geophones alone. Geophones are known to have a natural frequency of 10 Hz which limits their ability to sense the frequency content below, and broadband seismometers are too expensive for many applications. In Addition, downhole wireline geophones that can record transmission data require well intervention which is associated with considerable costs.

The rise of distributed acoustic sensing (DAS) offers a cost-effective way to fill this data gap as DAS measures seismically induced strain along the tangent of certain cable intervals down to frequencies below 1 Hz. DAS also provides a cost-effective way to densely sense the wavefield at greater depth by cementing the fiber optic cable into the well, and therefore can record transmission data without well intervention. The drawback of DAS measurements is that they often show a lower signal-to-noise ratio and solely provide one-dimensional strain measurements along the fiber tangent (Willis et al., 2016).

These distinct properties of geophone and fiberoptic data suggest that a combination of both data types can be exploited to improve EFWI imaging through enhanced acquisition geometries and extended sensing bandwidth. However, when simultaneously inverting both data types using EFWI, challenges related to the formulation of the data inclusion and the balancing of the data arise.

Theory

EFWI (Tarantola, 1986) is an inversion approach that reconstructs elastic properties more accurately than conventional imaging techniques, as the entirety of the recorded waveform is utilized. It is defined as an optimization problem that seeks a set of model parameters $\mathbf{m_{min}}$ which minimizes the data residuals between the resulting simulated data $\mathbf{d}^{\mathrm{pre}}$ and some observed data $\mathbf{d}$ (Tarantola, 1984a; Virieux and Operto, 2009):

$$\mathbf{m_{min}} = \min_{\mathbf{m}} \left(\sum_{i}^{N_F} \sum_{j}^{N_S} \frac{1}{2} \left\| \mathbf{W_i} \left(\mathbf{d}_{i,j} - \mathbf{d}_{i,j}^{\mathrm{pre}}(\mathbf{u}(\mathbf{m})) \right) \right\|^2 \right), \tag{1}$$

where $\mathbf{u}$ is the simulated wavefield based on the elastic parameter set $\mathbf{m}$ and it fulfills the 2D isotropic elastic wave equation in the frequency domain for every frequency i and every source j. $\mathbf{W_i}$ is a diagonal data weighting matrix which scales the data residuals. DAS data is incorporated in its native form via the formulation of a frequency-dependent sampling matrix $\widetilde{\mathbf{R}}_\mathbf{i}$ which is designed after Eaid et al. (2020):

$$\widetilde{\mathbf{R}}_\mathbf{i} = \begin{bmatrix} \widetilde{\mathbf{R}}_\mathbf{i}^{\mathbf{GP}} \\ \text{------} \\ \widetilde{\mathbf{R}}_\mathbf{i}^{\mathbf{DAS}} \end{bmatrix}, \qquad \text{with } \widetilde{\mathbf{R}}_\mathbf{i}^{\mathbf{GP}} = \begin{bmatrix} \cdots & 1\,0 & \cdots & & \\ \cdots & 0\,1 & \cdots & & \\ & \vdots & & & \\ & \cdots & 1\,0 & \cdots & \\ & \cdots & 0\,1 & \cdots & \end{bmatrix}, \tag{3a}$$

$$\text{and } \widetilde{\mathbf{R}}_\mathbf{i}^{\mathbf{DAS}} = \begin{bmatrix} \cdots & w_1\,w_2 & \cdots & w_3\,w_4 & \cdots & w_6\,w_5 & \cdots & w_7\,w_8 & \cdots \\ & & & \vdots & & & & & \\ \cdots & w_1\,w_2 & \cdots & w_3\,w_4 & \cdots & w_6\,w_5 & \cdots & w_7\,w_8 & \cdots \end{bmatrix}. \tag{3b}$$

The predicted data is then generated as

$$\mathbf{d}_{i,j}^{\mathrm{pre}}(\mathbf{u}(\mathbf{m})) = \widetilde{\mathbf{R}}_i\, \mathbf{u}_{i,j}(\mathbf{m}). \tag{4}$$

As seen, the upper part of the adjusted sampling matrix $\widetilde{\mathbf{R}}_\mathbf{i}$ generates geophone data by directly sampling the displacement at a given receiver location, while the lower part accounts for the strain measurements of the DAS at a given channel location. The latter creates one measurement based on a weighted sum of eight surrounding displacements. These weights w_1-w_8 account for the strain calculation on a staggered grid as well as gauge length effects (i.e. averaged fiber sensitivities) at every DAS channel location. Note that $\mathbf{W_i}$ needs to be adjusted such that geophone and DAS data residuals are of comparable magnitude. It also applies a trade-off parameter τ which can be used to increase the importance of one data type within the FWI procedure.

Method

Effects and benefits of frequency dependent DAS data inclusion within EFWI are illustrated using synthetic data of a fictional CO_2 sequestration scenario in which CO_2 is injected in two different reservoirs. Elastic models are derived from petrophysical subsurface models via the stiff-sand model following the procedure described in Hu et al. (2023). Data is created using 26 surface sources and 50 surface, multi-component geophones alongside a straight DAS fiber cemented to

the deviated injection well, which simulates a cost-effective acquisition scenario. DAS data is simulated from 2-70 Hz while geophone data is limited to 10 Hz at the low-frequency end. Different trade-off parameters and data balancing strategies are tested to identify challenges and potential mitigation strategies.

Results

As seen in Figure 1, EFWI results derived from only DAS or geophone data show poor model reconstruction as the individual datasets lack reflection and transmission data, respectively. A combination of both data types with a ratio of 1:3 (i.e. 25% DAS data weighting) provides improved balance, resulting in more accurate models and improved data fitting. Note that results in Figure 1 are derived from 10-70 Hz data that is available for both data types.

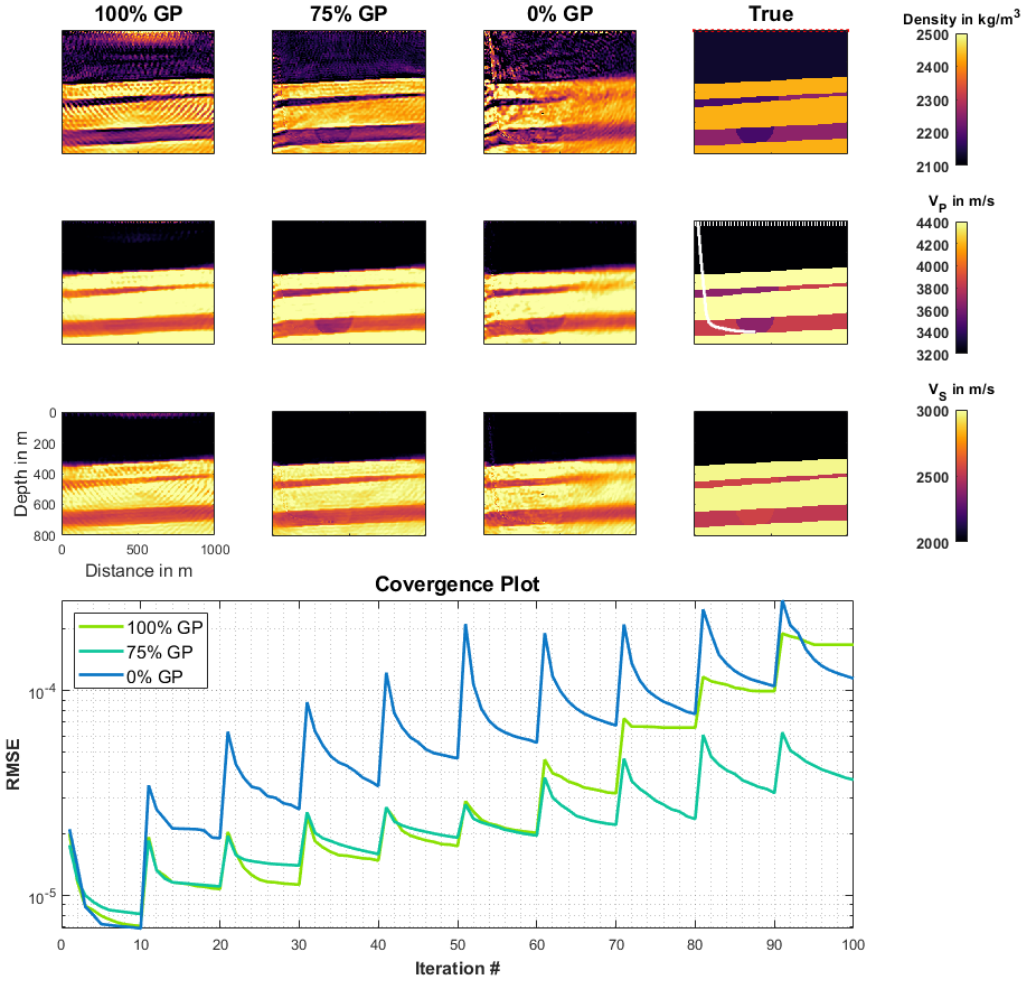

FIG. 1. EFWI comparison for different trade-off parameters τ. The upper section of the figure shows the final elastic parameter distributions after EFWI of only geophone data (left), 75% geophone and 25% DAS data (middle left), only DAS data (middle right) and the true models (right). At the bottom, the root-mean-square error (RMSE) throughout the EFWI procedures is shown. Sources (red) are indicated on the true density model, and geophone and DAS channel locations (white stripes and dots) are depicted on the true P-wave velocity model.

Frequency dependent DAS data inclusion (i.e. only DAS data available below 10 Hz) are presented in Figure 2. Two weighting strategies are tested to balance the DAS data below 10 Hz, namely (1) an adjustment of τ to 100% DAS data since all data at those frequencies belong to DAS, and (2) the same τ for all frequencies. The results indicate that weighting strategy 1 puts too much emphasis on DAS only frequencies such that data fit is deteriorated, and models appear smoothed out. Downweighing of those frequencies improves both of those aspects. In comparison to the 10-70 Hz inversion result slight improvements can be identified such as improved imaging on the left edge of the model.

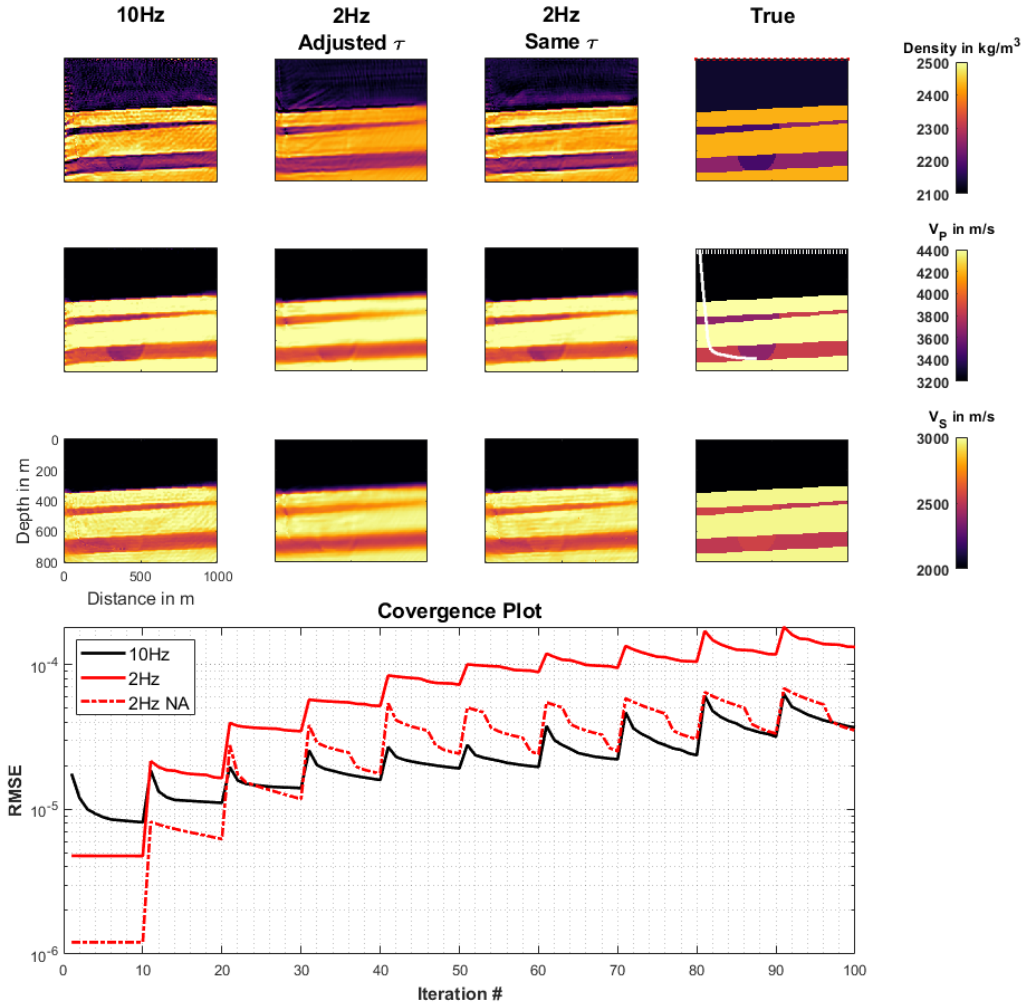

FIG. 2. EFWI comparison for different weighting strategies. The upper section of the figure shows the final elastic parameter distributions corresponding to the 10-70Hz and 2- 70Hz frequency bands, alongside the true models. "Same τ" indicates that the importance weighting is not adjusted, i.e. DAS data below 10Hz has importance of 25%, otherwise DAS is weighted with 100% for those frequencies. Sources (red) are indicated on the true density model, and geophone and DAS channel locations (white stripes and dots) are depicted on the true P-wave velocity model.

Conclusions

Simultaneous DAS-geophone EFWI has great potential to overcome issues related to wavefield sensing, frequency bandwidth and convergence behavior, however, it also poses challenges like the data balancing and data weighting. The results illustrate that these have significant influence on the result and proper testing of those parameters are required. Further challenges are expected when moving to field measurements as DAS data quality and data processing pose additional difficulties.

Acknowledgements

The sponsors of CREWES are gratefully thanked for continued support. This work was funded by CREWES industrial sponsors, and NSERC (Natural Science and Engineering Research Council of Canada) through the grant CRDPJ 543578-19. Further support of this work was provided by Emissions Reduction Alberta through the ACT4-SPARSE project. The first author of this report was supported by scholarships from the University of Calgary and the CSEG Foundation, which is gratefully acknowledged.

References

Bunks, C., Fatimetou, S., Zaleski, M., and Chavent, G., 1995, Multiscale seismic waveform inversion: GEOPHYSICS, 60, No. 5, 1457–1473.

Eaid, M. V., Keating, S. D., and Innanen, K. A., 2020, Multiparameter seismic elastic full-waveform inversion with combined geophone and shaped fiber-optic cable data: GEOPHYSICS, 85, No. 6, R537–R552.

Tarantola, A., 1984a, Inversion of seismic reflection data in the acoustic approximation: GEOPHYSICS, 49, No. 8, 1259–1266.

Tarantola, A., 1984b, Linearized Inversion of Seismic Reflection Data: Geophysical Prospecting, 32, No. 6, 998–1015.

Tarantola, A., 1986, A strategy for nonlinear elastic inversion of seismic reflection data: GEOPHYSICS, 51, No. 10, 1893–1903.

Virieux, J., and Operto, S., 2009, An overview of full-waveform inversion in exploration geophysics: GEOPHYSICS, 74, No. 6, WCC1–WCC26.

Willis, M. E., Erdemir, C., Ellmauthaler, A., Barrios, O., and Barfoot, D., 2016, Comparing DAS and Geophone Zero-Offset VSP Data Sets Side-By-Side: CSEG RECORDER Magazine, 41, 22–26.